CHEMISTRY OF MATERIALS
Review

Chem. Mater. **2011,** *23,* 621–630 621
DOI:10.1021/cm1024052

Multifunctional Materials in High-Performance OLEDs: Challenges for Solid-State Lighting[†]

Hisahiro Sasabe* and Junji Kido*

Department of Organic Device Engineering, Yamagata University, 4-3-16 Jonan, Yonezawa, Yamagata 992-8510, Japan

Received August 20, 2010. Revised Manuscript Received November 10, 2010

Recent advances in material chemistry have enabled white organic light-emitting device (OLED) efficacy beyond fluorescent tube efficacy up to 100 lm W^{-1}. In this short review, we explore recent developments of small molecule-based multifunctional materials in high-performance OLEDs, especially blue phosphorescent emitters, host materials, and electron-transporting materials.

1. Introduction

Nearly two decades have passed since the development of the first white organic light-emitting device (OLED) by Kido and co-workers.[1,2] Although the power efficacy of this white OLED was reportedly only <1 lm W^{-1}, researchers have reported the efficacy up to 100 lm W^{-1}, which is comparable to that of a fluorescent tube.[3−5] White OLEDs are mercury-free illumination light source and meet the requirements of the EU WEEE & RoHS directives, and hence, are one of the most promising candidates for energy-saving solid-state lighting and eco-friendly flat-display panels.[6,7] They are particularly useful where lightweight illumination devices are required, such as in aircraft and space shuttles, and are expected to usher in an era of new lighting designs, such as transparent lighting panels and luminescent wallpapers.

The primary requirements for a general-illumination light source are 3-fold: (1) power efficiency at high brightness (3000−5000 cd m^{-2}), which is greater than that of a fluorescent tube (>70 lm W^{-1}); (2) color rendering index (CRI) >80; (3) operational stability $>10\,000$ h at high-brightness.[8−13] To meet these requirements, the use of phosphorescent OLED technology is imperative, because phosphorescent emitters such as $Ir(ppy)_3$ and FIrpic (Figure 1) enable an internal efficiency as high as 100%, converting both singlet and triplet excitons into photons, and make OLED efficacy 4 times higher than that with fluorescent emitters.[14,15]

Two practical approaches exist for fabricating white OLEDs using phosphorescent emitters. One approach is to combine a blue fluorescent emitter with phosphorescent emitters of the other colors, creating a so-called hybrid white OLED.[16] The main requirement of this approach is the use of a blue fluorescent emitter with higher triplet energy (E_T) than that of the other phosphorescent emitters. The blue fluorescent emitter also needs to have a high photoluminescent quantum yield (η_{PL}). Several such hybrid white OLEDs have been developed. Schwartz and co-workers reported hybrid white OLED with a power efficiency at 1000 cd m^{-2} ($\eta_{p,1000}$) of 22 lm W^{-1} by using 4P-NPD (Figure 1) as a blue fluorescent emitter, and $Ir(ppy)_3$ and $Ir(MDQ)_2(acac)$ as green and red phosphorescent emitters, respectively.[17] Most recently, Kondakova and co-workers reported hybrid white OLED with $\eta_{p,1000}$ of 30 lm W^{-1} by using MQAB (Figure 1) as a blue fluorescent emitter and $Ir(ppy)_2pc$ as a yellow phosphorescent emitter.[18] In these hybrid OLEDs, a severe limitation is the development of a blue fluorescent emitter both with high E_T and η_{PL}, and at the present time, the $\eta_{p,1000}$s have been low around 30 lm W^{-1}. The other approach is to use all phosphorescent emitters to create a white OLED. Reineke and co-workers reported white OLED with fluorescent tube efficiency of 81 lm W^{-1} at 1000 cd m^{-2} by combining RGB phosphorescent emitters and light-outcoupling enhancement techniques, such as

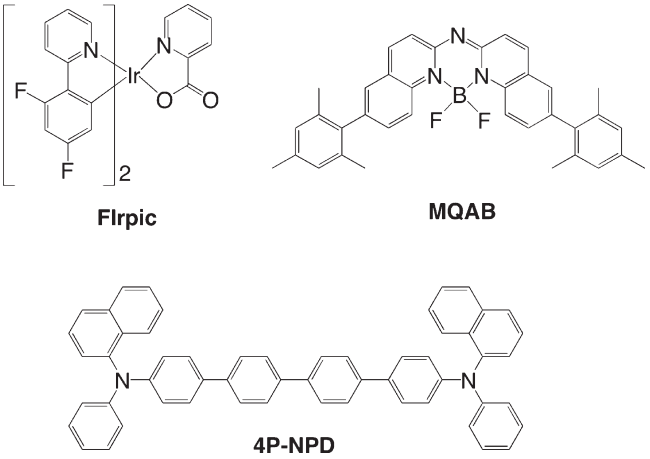

Figure 1. Blue phosphorescent emitter and fluorescent emitters in high-performance white OLEDs.

[†] Accepted as part of the "Special Issue on π-Functional Materials".

*Corresponding author. E-mail: h-sasabe@yz.yamagata-u.ac.jp (H.S.); kid@yz.yamagata-u.ac.jp (J.K.). Fax: (+81)-238-26-3412. Tel: (+81)-238-26-3052.

Published on Web 12/01/2010

use of high-refractive-index substrates and half-spheres.[4] However, the efficiency was decreased to $\eta_{p,1000}$ of 33 lm W^{-1} (EQE 14.4%) without light-outcoupling enhancement. On the other hand, Su and co-workers reported two-color white OLED with $\eta_{p,1000}$ of 44 lm W^{-1} (EQE 25%).[19] Thus, to realize a white OLED whose power efficiency exceeds that of a fluorescent tube, a key solution is to generate novel phosphorescent materials.

In material synthesis for small molecule-based phosphorescent OLEDs, researchers today are focusing mainly on the three areas: (1) blue phosphorescent emitters, (2) host materials, and (3) electron-transporting materials (ETL). In this short review article, we discuss recent advances in these three areas.

2. Multifunctional Materials in High-Performance OLEDs

2.1. Blue Phosphorescent Emitters. The efficacy of a white OLED strongly depends on the properties of the blue emitter contained therein. Thus, development of blue phosphorescent emitters and related materials is of paramount importance. In 2001, a sky-blue phosphorescent emitter called FIrpic, was synthesized and a blue OLED based on FIrpic was demonstrated.[20] In this device, a carbazole-based host material CBP was used as a host material. The power efficiency was repoted to be as low as 6.3 lm W^{-1} (EQE 5.7%), but the use of high E_T host materials CDBP and mCP gave improved efficacy of up to 10.5 lm W^{-1} (EQE 10.4%) (Figure 2).[21,22] These results indicate that high E_T host materials are critically important to confine the triplet exciton in the emissive layer (EML). However, the maximum EQE of this device remained at around 10%, which was much less than the theroretical limit of EQE. In 2005, we developed a FIrpic-based OLED with $\eta_{p,max}$ of 37 lm W^{-1} (EQE 19%) by using novel high E_T materials (Figure 3). This device used high E_T materials not only as a host but also as an ETL and hole-transporting material (HTL).[23] In 2008, we have realized a FIrpic-based OLED with $\eta_{p,max}$ over 60 lm W^{-1} (EQE 24%) using a wide-energy gap ETL.[24] These devices use high E_T HTLs and ETLs, which act as carrier-transporters as well as triplet exciton blockers to minimize the efficiency loss at HTL/EML and/or EML/ETL interface.

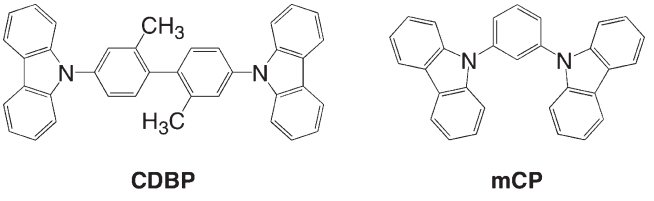

Figure 2. First-generation wide-energy-gap host materials.

Although FIrpic-based OLEDs were thereby improved, some limitations remained. For example, the blue phosphorescent emitters FIrpic and FIr6 have an emission maxima (λ_{em}) at 470 and 458 nm, respectively. However, the CRI of white OLEDs would be greatly improved by use of a pure blue emitters having λ_{em} at 450 nm. Hence, development of a pure blue emitters is necessary for realizing high-quality illumination light-sources. Moreover, FIrpic-based OLEDs have limited operational lifetimes, which could be improved by sophisticated device/material engineering.[25] Operational lifetimes differ for emitters of different colors, causing the color of a white OLED to change with time—a problem that is particularly detrimental for long-term lighting.[7,8] Thus, a key solution is to develop a stable, pure blue phosphorescent emitter and related materials.

A number of other types of blue phosphorescent emitters have been reported. For example, Chi and co-workers reported mixed-ligandated blue iridium complexes containing phenylpyridine, pyrazole, phosphine, and carbene ligands (Figure 4).[26−29] Tris-ligandated blue phosphorescent emitters, such as phenylpyridine-based FCNIr,[30] phenyltriazole-based Ir(taz),[31] bipyridine-based $Ir(dfpypy)_3$[32] and carbene-based mer-Ir(cn-pmic),[33] have also been reported (Figure 5).

OLEDs based on different types of blue phosphorescent emitters have also been reported, such as carbene-based blue OLED[33] with a $\eta_{p,max}$ as high as 12 lm W^{-1}, and FCNIr-based OLED[30] with $\eta_{p,max}$ of 17 lm W^{-1} (21.1 cd A^{-1}). However, these devices showed low efficacy below 10 lm W^{-1} at 100 cd m^{-2}. On the other hand, Universal Display Corporation and BASF have independently announced the development of blue phosphorescent emitters with improved lifetime,[34,35] although the chemical structures and the details about device structures were not disclosed. Thus, the issue of enhancing operational lifetime for blue phosphorescent OLEDs should be solved in the near future.

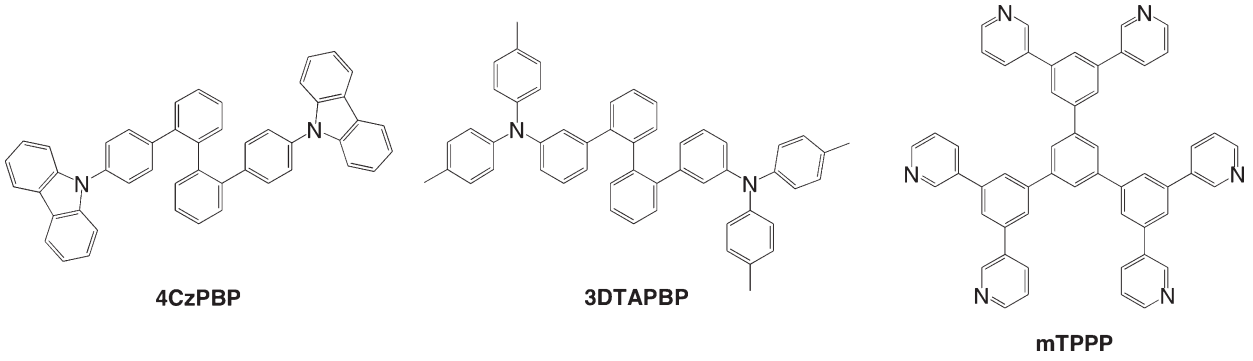

Figure 3. Wide-energy-gap materials in high-performance blue OLED.

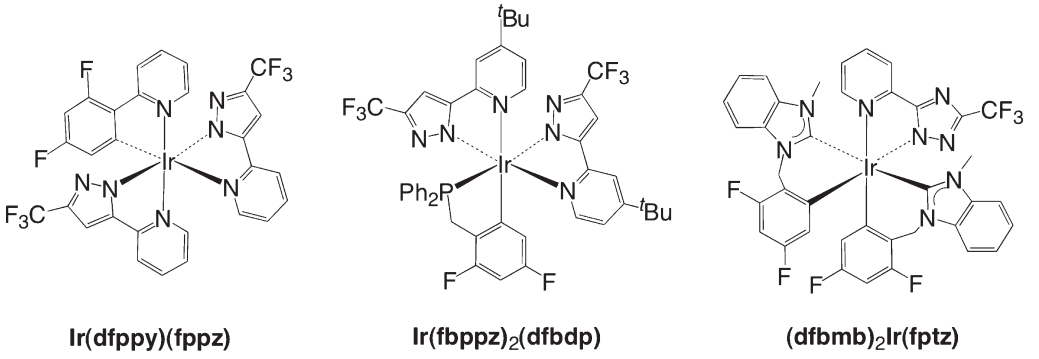

Figure 4. Examples of novel blue phosphorescent emitters with mixed ligand system.

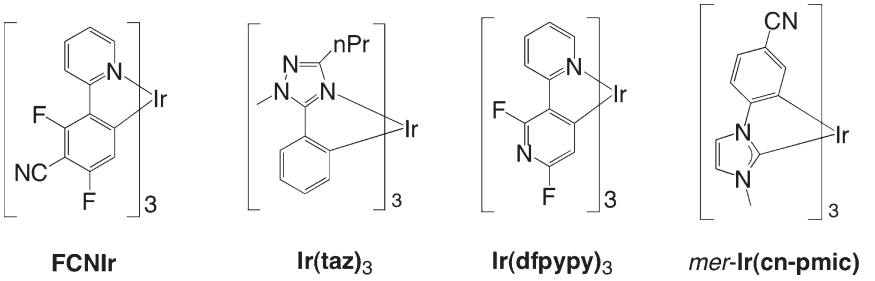

Figure 5. Examples of tris-ligandated blue phosphorescent emitters.

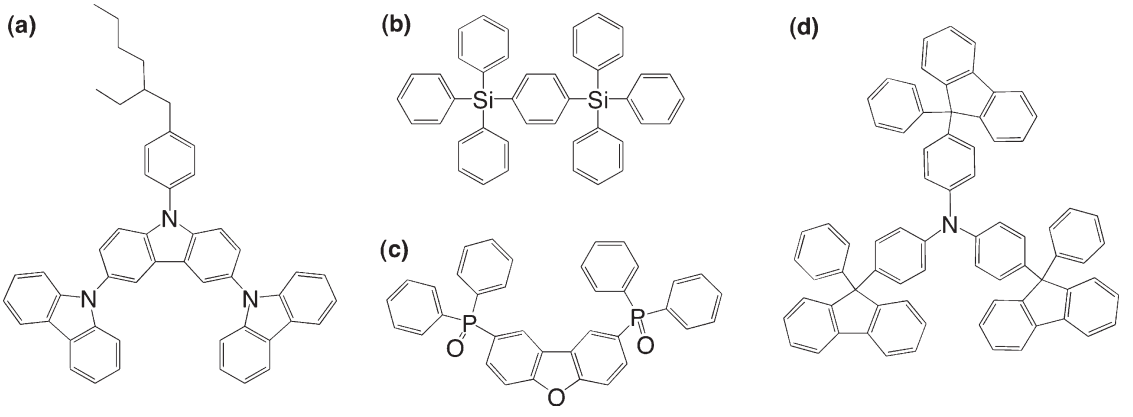

Figure 6. Representatives of wide-energy-gap host materials based on (a) carbazole, (b) tetraphenylsilane, (c) phosphine oxide, and (d) triphenylamine derivatives in FIrpic-based OLEDs.

2.2. Multifunctional Host Materials. Mi and co-workers recently provided an excellent review of host materials for RGB phosphorescent emitters.[36] Thus, in this section, we focus on only a few high-performing host materials in blue and white OLEDs, with emphasis on our laboratory results.

As mentioned above, the host materials for blue emitters play a critical role in determining the device performance. The primary requirements of phosphorescent host materials are (1) the confinement of the triplet excitons on the emitter, (2) the suppression of dopant aggregation, and (3) the adjustment of the carrier balance of holes and electrons in the EML. To meet these requirements from a material side, (a) carbazole-based host materials,[37−42] (b) tetraphenylsilane-based host materials,[43,44] (c) phosphine oxide-based host materials,[45−47] and (d) triphenylamine-based host materials[48] have been developed for FIrpic-based blue OLEDs (Figure 6). Of these, the carbazole derivatives are among the most attractive candidates for reducing OLED driving voltage because of their small singlet−triplet exchange energy ΔE_{ST}, which is attributed to the energy difference between the singlet excited energy E_{S1} and the E_T,[49] and their high chemical compatibility with dopants to suppress the dopant aggregation.[50]

In addition to the above requests from material side, researchers should take care of the requests from device side by preventing the major problem of efficiency roll-off, which is a typical phenomenon in phosphorescent OLEDs and indicates the significant efficiency decrease at high current densities.[51] To maintain the high-efficiency at high brightness (3000−5000 cd m^{-2}), which is typically accompanied by high current density, it is important to solve the efficiency roll-off problem. Reineke and co-workers recently pointed out that the efficiency roll-off caused by triplet−triplet annihilation (TTA)[52] is greatly influenced by the emitter aggregation in an $Ir(ppy)_3$-based OLED.[53,54]

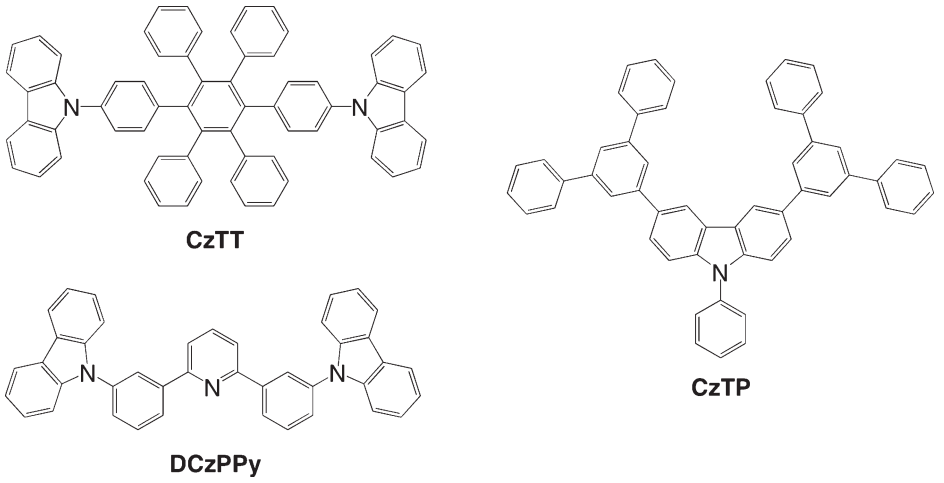

Figure 7. Examples of wide-energy-gap host materials in FIrpic-based OLEDs.

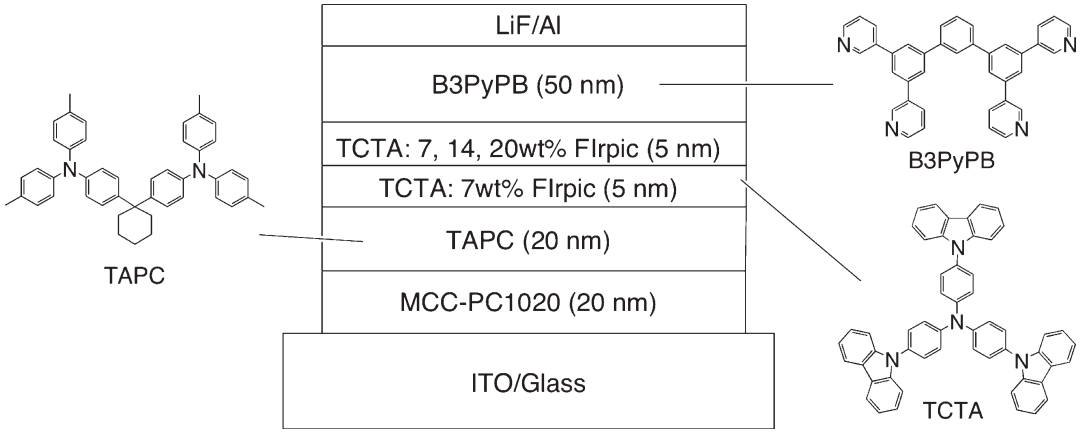

Figure 8. Device architecture and materials used in high-performance FIrpic-based OLED.

Emitter aggregation also causes the significant loss of η_{PL}. Giebink and Forrest reported that efficiency roll-off at current density < 1000 mA cm^{-2} is caused by loss of carrier balance in phosphorescent OLEDs with the short-radiative-lifetime emitters.[55] These two reports clearly indicate that the problem of efficiency roll-off can be solved by maintaining carrier balance, suppressing emitter aggregation, and using short-radiative-lifetime emitters such as $Ir(ppy)_3$ and FIrpic. Promising approaches to maintain carrier balance to employ a double EML strategy[56] and insert wide-energy-gap HTL and ETL as carrier blockers. By using good solubilizing host material for emitters, aggregation and TTA issues can be minimized.

We recently synthesized four new carbazole-based host materials, 4CzPBP,[57] CzTT,[58] CzTP,[59] and DCzPPy[60] (Figure 7). The first three of these host materials performed well in FIrpic-based OLEDs with $\eta_{p,max}$ of up to 55 lm W^{-1} (EQE 23%). The fourth, DCzPPy performed exceptionally well in combination with TCTA in blue and white OLEDs.[19,60] In a FIrpic-based OLED, efficiency roll-off was significantly reduced at high brightness even though the total EML thickness was only 10 nm. We evaluated the efficiency roll-off by examining its current density $J_{1/2}$ at half the maximum EQE; for the DCzPPy device, $J_{1/2} = 82$ mA cm^{-2}.[19] This value is exceptionally large for phosphorescent OLEDs, probably due to excellent carrier/exciton confinement. In addition, effective hole and electron injections create a well-balanced carrier that remains constant even at high brightness. This favorable effect can be attributed to presence of a pyridine moiety with an electron-deficient C=N double bond at the center of the host molecule. We speculate that the weak electron-accepting nature of the pyridine moiety promotes electron-injection as well as electron-transport. Indeed, the superior electron-transporting nature of DCzPPy has been demonstrated in performance comparisons of an ITO/NPD/DCzPPy/Alq/LiF/Al device and a CBP device.[60] Fukagawa and co-workers reported a similar effect for a pyridoindole derivative in a blue OLED.[61] In this case, the pyridoindole moiety with a C=N double-bond can be regarded to be an aza analog of a carbazole, and shows superior electron-transporting property compared to UGH2.

A commercially available material TCTA can be used in FIrpic-based OLEDs. A OLED incorporated with TCTA/FIrpic as EMLs has been reported (Figure 8).[24,62,63] The two EMLs of this OLED use a single host TCTA, and only FIrpic concentration is varied. The device structure is [ITO/MCC-PC1020 (20 nm)/TAPC (20)/TCTA: 7 wt % FIrpic (5 nm)/TCTA: 7, 14, 20 wt %

FIrpic (5 nm)/B3PyPB(50 nm)/LiF/Al]. The power efficiency−luminance characteristics is shown in Figure 9. In this architecture, higher FIrpic doping concentration improves device performance, probably because of the higher carrier balance achieved by improved ETL-to-EML electron-injection. The optimized device shows $\eta_{p,max}$ over 60 lm W^{-1} (EQE 24%) and $\eta_{p,1000}$ of 42 lm W^{-1} (EQE 21%).

2-3. Multifunctional Electron-Transporting Materials. Multifunctional ETLs have also been reported. For small molecule-based OLEDs, silole, oxadiazole, and triazole derivatives as well as metal complexes have been synthesized and investigated as attractive ETL candidates for use in fluorescent OLEDs (Figure 10).[64,65] However, for use in green or blue phosphorescent OLEDs, the E_T levels of most of these materials are too low to block exciton diffusion; hence, this results in significant efficiency loss. For example, the pyridine-containing silole derivative PyPySPyPy is known to be an excellent ETL with high electron mobility ($\mu_e = 2 \times 10^{-4}$ cm^2 V^{-1} s^{-1}).[66,67] However, in a green phosphorescent OLED, its power efficiency was much lower than that of BCP.[68] This can be attributed to its poor hole-blocking ability and low E_T level. For use in blue phosphorescent emitters, even BCP and TAZ are unsuitable due to their low E_T levels. In addition, for low-cost manufacturing, device architecture should be simple. Therefore, development of an ETL having the following functionalities is important: (1) high electron injection property, (2) high μ_e, (3) high hole-blocking ability, and (4) high E_T level to block exciton diffusion.

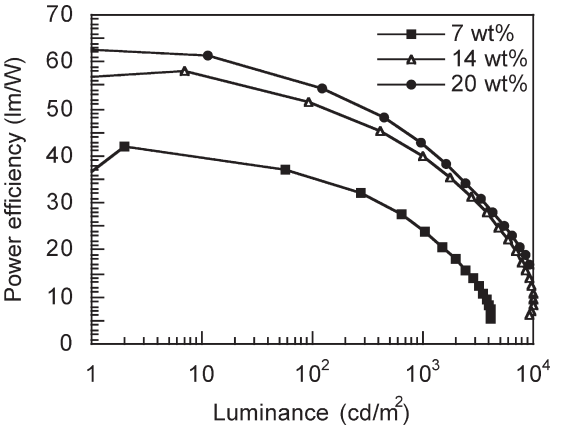

Figure 9. Power efficiency−luminance characteristics in FIrpic-based OLED with B3PyPB.

Pyridine-containing ETLs (other than some silole derivatives) have received comparatively less attention than have the above-mentioned ETLs, according to a 2004 review article in Chemistry of Materials.[64] We developed a number of pyridine-containing ETLs.[19,22,24,69−79] These ETLs offer many advantages, such as high thermal stability (T_g > 100 °C), high hole-blocking ability, high E_T level (>2.77 eV) to block triplet exciton diffusion, and high μ_e (up to 1×10^{-3} cm^2 V^{-1} s^{-1} order). By using a combination of phosphorescent emitters such as FIrpic and $Ir(ppy)_3$, we developed high-efficiency sky-blue,[24] green,[71,72] orange-red[80] and white[19] OLEDs with EQEs of up to 29%. The use of outcoupling enhancement such as high-refractive-index substrates and half-spheres should more than double this EQE value.[4,81]

As Jenekhe and co-workers, in their earlier review, pointed out the importance of "structure-μ_e relationships that could guide the design of next-generation ETLs."[64] Thus, detailed studies of the relationships among material structure, physical property, and device performance are still important. Only a few sets of ETLs are presently available for such studies.

Several ETLs have been investigated to determine the effect of the core skeleton on I_p and E_a, physical properties

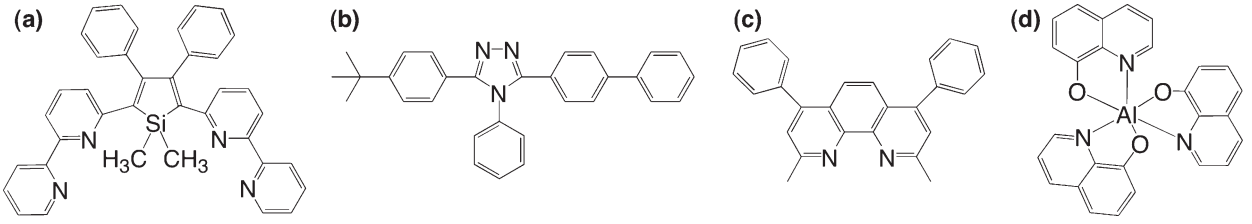

Figure 10. Representative example of electron-transporting materials based on (a) silole, (b) triazole, (c) phenanthroline, and (d) metal complex derivatives.

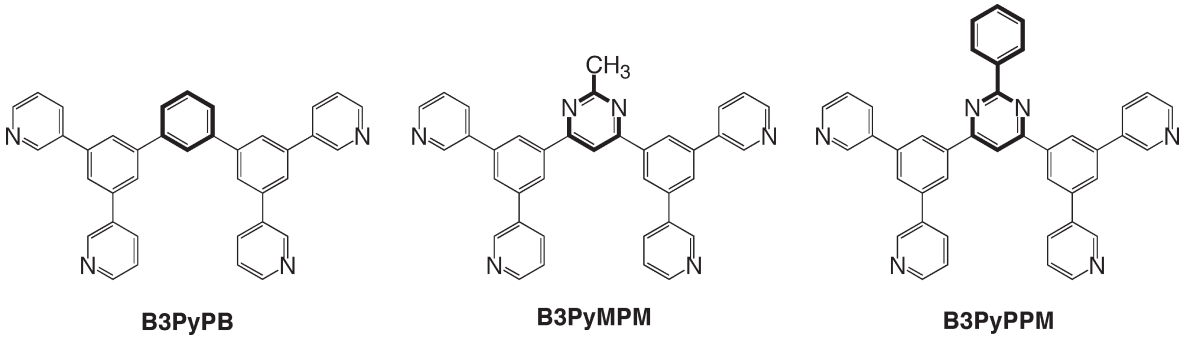

Figure 11. Series of ETLs with 3,5-dipyridylphenyl moieties.

and OLED performance. For ETLs containing 3,5-dipyridylphenyl moieties, replacing the benzene skeleton with 2-methylpyrimidine or 2-phenylpyrimidine changes I_p from 6.7 to 7.2 eV and E_a from 2.6 to 3.7 eV (Figure 11 and Table 1).[24,62,63,72] Ir(ppy)$_3$-based OLEDs with different ETLs, i.e., B3PyPB, B3PyPPM and as a reference, BCP/Alq, have been reported.[63] The device structure is [ITO/TPDPES: 10 wt % TBPAH (20 nm)/TAPC (30)/CBP: 8 wt % Ir(ppy)$_3$ (10 nm) /ETL (50 nm)/LiF/Al]. The power efficiency−luminance characteristics is shown in Figure 12. B3PyPB- and B3PyPPM-based OLEDs show superior performance with $\eta_{p,max}$ of 118 lm W^{-1} (29%) and 140 lm W^{-1} (29%), respectively, which is approximately 1.5−1.7 times higher than the value for the reference (Table 2). Operating voltage is much lower for a B3PyPPM-based OLED than for a B3PyPB-based OLED (2.6 and 3.2 V, respectively, at 100 cd m^{-2}), even though μ_e for B3PyPPM is 1/1000 lower than for B3PyPB.[24,72] Such reduced operating voltage is attributed to deeper E_a level of B3PyPPM. Thus introduction of a pyrimidine-skeleton with two C=N double-bonds greatly enhances electron-injection property.

Table 1. Comparison of Physical Properties of ETLs with 3,5-Dipyridylphenyl Moieties

compd	I_p (eV)	E_a (eV)	E_g (eV)	μ_e (cm^2 V^{-1} s^{-1})
B3PyPB	6.67	2.62	4.05	1×10^{-4}
B3PyMPM	6.97	3.44	3.53	1×10^{-5}
B3PyPPM	7.15	3.74	3.41	1×10^{-7}

Table 2. Summary of Ir(ppy)$_3$-Based OLED Performances

ETL	$\eta_{p,max}/\eta_{c,max}$ (lm W^{-1}/cd m^{-2})	$\eta_{p,100}/\eta_{c,100}$ (lm W^{-1}/cd m^{-2})	$\eta_{p,1000}/\eta_{c,1000}$ (lm W^{-1}/cd m^{-2})
BCP/Alq	82/84	63/79	42/67
B3PyPB	118/105	104/102	76/89
B3PyPPM	140/98	126/103	96/93

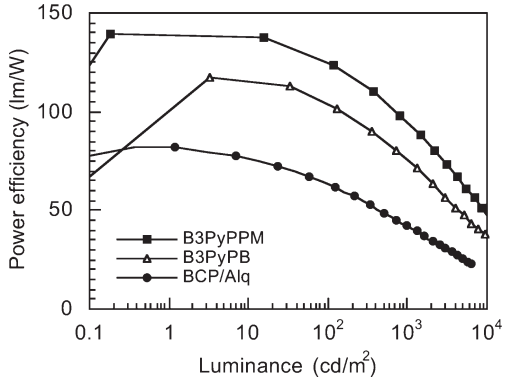

Figure 12. Power efficiency−luminance characteristics in Ir(ppy)$_3$-based OLED with BCP/Alq, B3PyPB and B3PyPPM.

Similarly, Su and co-workers investigated structure−property relationships for TmPyPB derivatives, and reported that the orientation of nitrogen on the peripheral pyridines affects electron injection properties and OLED performances (Figure 13).[75] For FIrpic-based OLEDs, performance, as measured by the current density and luminance at the same voltage, decreases in the order Tm4PyPB > Tm3PyPB > Tm2PyPB. For TmPyPB derivatives, E_a levels decreases in the order Tm4PyPB (2.94 eV) > Tm3PyPB (2.90 eV) > Tm2PyPB (2.74 eV) as predicted by the DFT calculation. The measured values of μ_e are all of nearly the same order of 10^{-3} cm^2 V^{-1} s^{-1} irrespective of nitrogen orientation. Thus, we deduce that differences in OLED performance are due to the different electron-injection natures of the TmPyPB derivatives.

Leo and co-workers reported that the theoretical voltage required to reach 100 cd m^{-2} for a green OLED is 1.95 V.[82] This value is significantly lower than operating voltages observed to date, so it is still desirable to try to reduce operating voltage. As mentioned above, in a series of ETLs containing the 3,5-dipyridylphenyl moiety, the core skeleton plays a critical role in determining I_p and E_a levels. A promising approach to lowering E_a level is to introduce an electron-deficient aromatic group at the center of the molecule. Among aza-aromatic compounds, triazine with three C=N double-bonds is known to have a lower E_a level than pyrimidine. Su and co-workers recently showed experimentally that a triphenyltriazine-skeleton-based ETL lowers the turn-on voltage at 1 cd m^{-2} of an Ir(ppy)$_3$-based OLED to an extremely low at 2.2 V and achieves a driving voltage of 2.4 V at 100 cd m^{-2} (Figure 14).[79] This result clearly indicates that ideal operating voltages can be realized using an appropriately designed ETL without *n*-doping,[83−85] and that a relatively large barrier exists at the EML/ETL interface as well as at the ETL/cathode interface. To gain more insight into the origin of electron-transporing properties, a fundamental understanding of the structural parameters is necessary.

We recently prepared three types of ETLs−B2PyMPM, B3PyMPM and B4PyMPM−to investigate the effect of nitrogen orientation on physical properties. Each ETLs has a different nitrogen orientation on the peripheral pyridine rings (Figure 15).[86] The value of T_m for B4PyMPM is

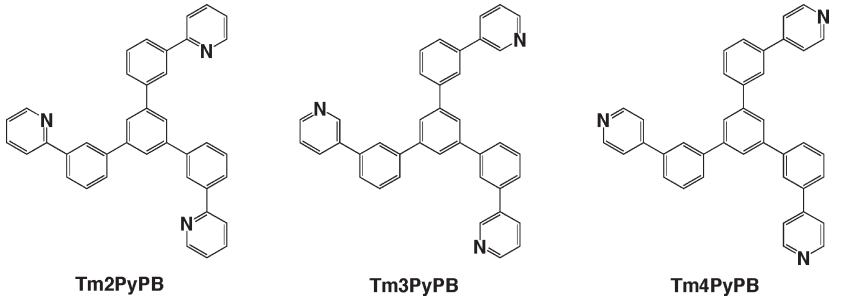

Figure 13. Chemical structures of Tm2PyPB, Tm3PyPB, and Tm4PyPB.

estimated to be approximately 50 °C higher than that for B3PyMPM, and approximately 120 °C higher than that for B2PyMPM (Table 3). Because the only difference in these derivatives is the nitrogen orientation, these results may be mainly due to the CH−N hydrogen-bond interactions in the solid state. The degree of these interactions increases in the order B2PyMPM < B3PyMPM < B4PyMPM. The I_p levels increases in the order B2PyMPM (6.62 eV) < B3PyMPM (6.97 eV) < B4PyMPM (7.30 eV), as measured by using an ultraviolet photoelectron spectroscopy. Thus, the effect of the peripheral pyridine rings on I_p is relatively small compared to the effect of the core skeleton on I_p.

The time-of-fight measurements of vacuum-deposited films have also been carried out. At room temperature, μ_e for B4PyMPM is reportedly 10 times higher than that for B3PyMPM and 100 times higher than that for B2PyMPM (Figure 16).

To determine the charge-transport parameters for the BPyMPM derivatives, we investigated the temperature and field dependencies of μ_e by using Bässler's disorder formalism. The values of the electron-transport parameters are listed in Table 4. The degree of energetic disorder σ, which describes fluctuations of the hopping site energy, is estimated to decrease in the order B2PyMPM (91 meV) > B3PyMPM (88 meV) > B4PyMPM (76 meV). In BPyMPM derivatives, because the number of conformers increases in the order B4PyMPM < B3PyMPM = B2PyMPM, the differences in σ can be attributed mainly to the number of conformers. The value of positional disorder Σ, which describes fluctuations of the intermolecular distance, is calculated to be 2.7 for B2PyMPM, and <1.5 for B3PyMPM and B4PyMPM. Thus, because μ_0 for B4PyMPM is relatively large, partially well-ordered molecular orientations should be obtainable in a vacuum-deposited B4PyMPM film.

In 2007, Winkler and Houk computationally predicted that nitrogen-rich oligoacenes can form self-complementary systems to make highly ordered 2D sheets by means of intermolecular CH−N hydrogen-bond interactions (Figure 17).[87] Although CH−N hydrogen bonds are relatively weak, the large number of contacts is expected to facilitate formation of 2D sheets in a self-complementary system. In addition, Ziener and co-workers determined by using scanning tunnel microscopy that an oligopyridine derivative can be assembled into 2D sheets at the liquid/solid interface on highly oriented pyrolytic graphite (HOPG) (Figure 18).[88,89] This oligopyridine derivative has a very similar structure of BPyMPM derivatives. Considering the results of electron-transport parameters of BPyMPM derivatives, we hypothesize that vacuum-deposited B3PyMPM and B4PyMPM films have partially well-ordered molecular orientations as well as dense packing derived from the CH−N hydrogen-bond interactions leading to high μ_e (Figure 19). To confirm this hypothesis, it is necessary to investigate molecular aggregation states.[90,91]

Table 3. Comparison of Physical Properties of 2-Methylpyrimidine Skeleton-Based ETLs

compd	I_p (eV)	E_a (eV)	E_g (eV)	T_m (°C)
B2PyMPM	6.62	3.07	3.55	257
B3PyMPM	6.97	3.44	3.53	326
B4PyMPM	7.30	3.71	3.59	374

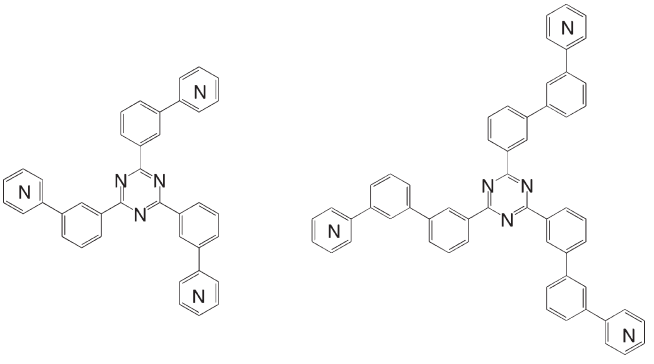

Figure 14. Chemical structures of triphenyltriazine skeleton-based ETLs. Reproduced with permission from ref 79. Copyright 2010 Wiley-VCH Verlag GmbH & Co. KGaA.

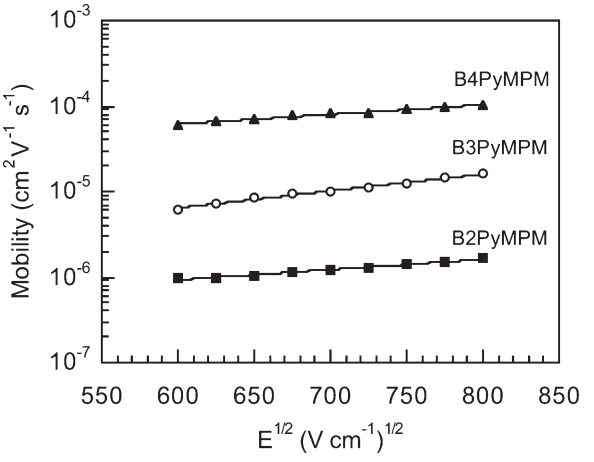

Figure 16. Electron mobility of BPyMPM derivatives by TOF measurement at room temperature. Reproduced with permission from ref 86. Copyright 2010 Wiley-VCH Verlag GmbH & Co. KGaA.

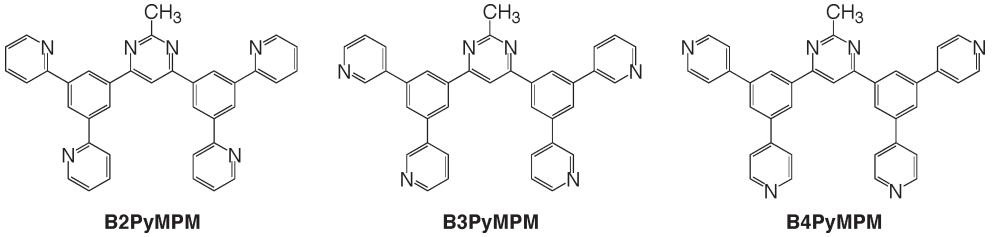

Figure 15. Chemical structures of 2-methylpyrimidine skeleton-based ETLs. Reproduced with permission from ref s86. Copyright 2010 Wiley-VCH Verlag GmbH & Co. KGaA.

Similarly, intramolecular CH−N hydrogen-bond interactions also enhances the mobility of a molecule due to induced structural planarity. Yokoyama and co-workers have investigated the molecular aggregation state of oxadiazole derivatives[92] by a variable angle spectroscopic ellipsometry.[93] They reported that intramolecular CH−N hydrogen-bond interactions of pyridine rings cause the molecules to become planar and enhance the horizontal molecular orientation, leading to high mobility.

Table 4. Electron-Transport Parameters of 2-Methylpyrimidine Skeleton-Based ETLs

compd	μ_e ($cm^2\ V^{-1}\ s^{-1}$)[a]	μ_0 ($cm^2\ V^{-1}\ s^{-1}$)[b]	σ (meV)[c]	Σ[d]
B2PyMPM	1.6×10^{-6}	5.1×10^{-6}	91	2.7
B3PyMPM	1.5×10^{-5}	6.9×10^{-5}	88	1.2
B4PyMPM	1.0×10^{-4}	4.5×10^{-4}	76	0.6

[a] Mobility at room temperature. [b] Hypothetical mobility in the disorder-free system. [c] Energetic disorder. [d] Positional disorder.

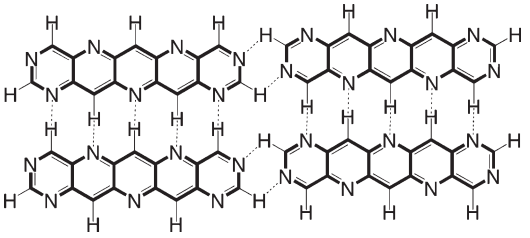

Figure 17. Proposed network formation based on weak CH-N hydrogen-bonding interaction. Reprinted with permission from ref 87. Copyright 2007 American Chemical Society.

As mentioned above, it is important to control the 2D and 3D molecular-aggregation states for development of next-generation multifunctional ETLs—for example, by means of weak intra- and/or intermolecular hydrogen-bond interactions.[94] Researchers in the field of organic electronics will require supramolecular solid-state views to create novel multifunctional materials.

3. Conclusion and Outlook

In this short review, we described recent advances in multifunctional materials designed for use in high-performance OLEDs. To realize performance levels beyond those of current fluorescent tubes, development of a long-life blue phosphorescent emitter and related materials is required. A joint study is needed to facilitate such development, and a study that includes contributions from quantum chemistry, material synthesis, and device physics would be ideal.[95−97] Organic materials offer flexibility in material design, and an unlimited number of organic materials can be synthesized. In early 2010, an OLED panel maker, Lumiotec (Yonezawa, Japan) started to ship sample OLED lighting with fluorescent materials.[98] In the near future, development of a stable blue phosphorescent emitter and use of multiphoton[99,100]

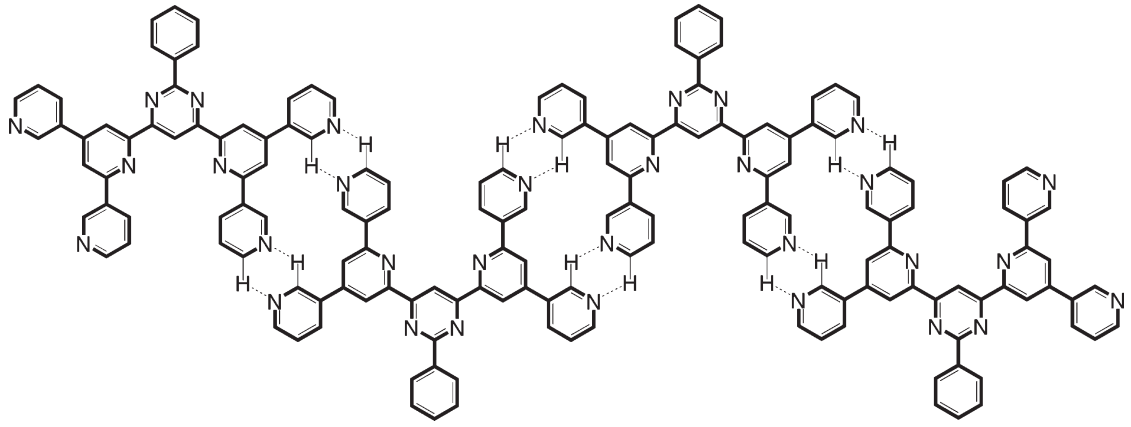

Figure 18. Formation of 2D sheet like structure based on weak CH-N hydrogen-bonding interaction. Reprinted with permission from ref 88. Copyright 2005 American Chemical Society.

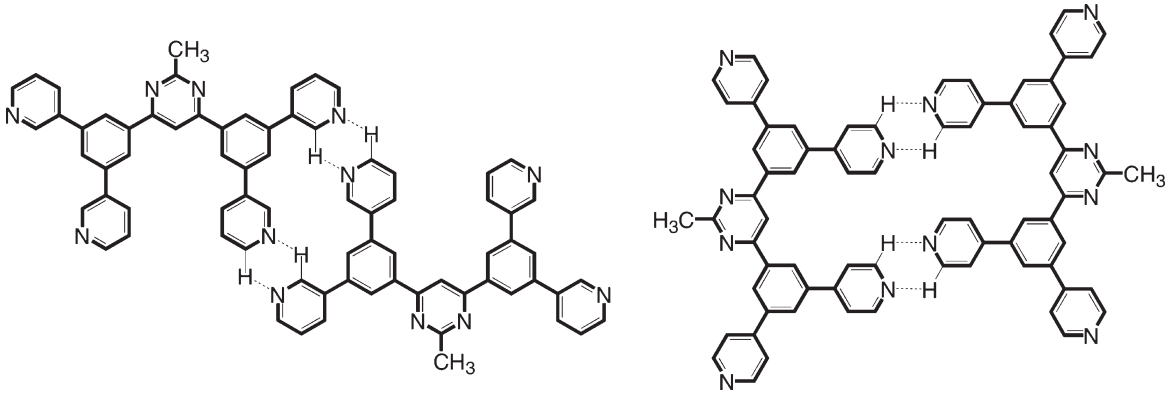

Figure 19. Examples of proposed network formation of B3PyMPM and B4PyMPM based on weak CH−N hydrogen-bonding interaction.

and/or graded structures,[101,102] should make the white OLED a real candidate for next-generation illumination light source. In addition, several pyridine-containing ETLs show not only outstanding performances but also possibly unique self-assembled natures in the solid state. Hence, their further study is important. Finally, as mentioned previously, only a limited set of ETLs is available to study the interrelationships among material structure, physical properties, and device performance. In addition, general guidelines for material design and device engineering are required to maximize device performance.

Research on high-performance OLEDs can help in development of not only industrial applications but also fundamental science. Creative chemists and co-workers from other fields should collaborate to open new possibilities in the field of organic electronics.

Acknowledgment. We would like to thank all the researchers who participated in the works discussed in the present paper and whose names appear in references. We also greatly acknowledge the financial support in part by New Energy and Industrial Technology Development Organization (NEDO) through the "Advanced Organic Device Project" and by Japan Regional Innovation Strategy Program by the Excellence (J-RISE) (Creating international research hub for advanced organic electronics) of Japan Science and Technology Agency (JST).

Acronyms Used

WEEE: Waste Electrical and Electronic Equipment Directive
RoHS: Restricting the use of Hazardous Substances in electrical and electronic equipment
$Ir(ppy)_3$: *fac*-tris(2-phenylpyridine)iridium(III)
FIrpic: iridium(III)bis(4,6-(difluorophenyl)pyridinato-$N,C^{2'}$)picolinate
4P-NPD:*N*,*N*′-di-1-naphthalenyl-*N*,*N*′-diphenyl-[1,1′:4′,1″:4″,1‴-quaterphenyl]-4,4‴-diamine
$Ir(MDQ)_2$(acac):iridium(III)bis(2-methyldibenzo-[*f*,*h*]-quinoxaline)(acetylacetonate)
MQAB:difluoro[6-mesityl-*N*-(2-(1H)-quinolinylidene-*kN*)-(6-mesityl-2-quinolinaminato-*kN*1)]boron
$Ir(ppy)_2$pc: *fac*-bis(2-phenylpyridine)(2-pyridylcoumarin)-iridium(III).
CBP: 4,4′-*N*,*N*′-dicarbazolylbiphenyl
CDBP: 4,4-bis(9-carbazolyl)-2,2-dimethyl-biphenyl
mCP: *N*,*N*-dicarbazolyl-3,5-benzene
4CzPBP: 2,2′-bis(4-carbazolylphenyl)-1,1′-biphenyl
3DTAPBP: 2,2′-bis[3″-(*N*,*N*′-ditolylamino)phenyl]-biphenyl
mTPPP: 1,3,5-tris[3,5-bis(pyrid-3-yl)phenyl]benzne
FIr6: iridium(III)bis(4′,6′-difluorophenylpyridinato)-tetrakis(1-pyrazolyl)borate
CzTT: 4,4″-dicarbazole-2′,3′,5′,6′-tetraphenyl-*p*-terphenyl
CzTP: 3,6-bis-[1,1′;3′1″]terphenyl-5′-yl-9H-carbazole
DCzPPy: 2,6-bis[3′-(*N*-carbazole)phenyl]pyridine
TCTA: 4,4′,4″-tris(N-carbazolyl)triphenylamine
TAPC: 1,1-bis[4-[*N*,*N*-di(*p*-tolyl)amino]phenyl]cyclohexane
B3PyPB: 3,5,3″,5″-tetra-3-pyridyl-[1,1′;3′,1″]terphenyl
BPyMPM: bis-4,6-(3,5-dipyridylphenyl)-2-methylpyrimidine
BPyPPM: 2-phenyl-4,6-bis(3,5-dipyridylphenyl)primidine
TmPyPB: 1,3,5-tri(m-pyridyl-phenyl)benzene

References

(1) Kido, J.; Hongawa, K.; Okuyama, K.; Nagai, K. *Appl. Phys. Lett.* **1994**, *64*, 815.
(2) Kido, J.; Kimura, M.; Nagai, K. *Science* **1995**, *267*, 1332.
(3) D'Andrade, B. W.; Esler, J.; Lin, C.; Adamovich, V.; Xia, S.; Weaver, M. S.; Kwong, R.; Brown, J. J. *Proc. SPIE* **2008**, *7051*, 70510Q-1.
(4) Reineke, S.; Lindner, F.; Schwartz, G.; Seidler, N.; Walzer, K.; Lüssem, B.; Leo, K. *Nature* **2009**, *459*, 234.
(5) Sun, Y.; Giebink, N. C.; Kanno, H.; Ma, B.; Thompson, M. E.; Forrest, S. R. *Nature* **2006**, *440*, 908.
(6) Yersin, H., Eds. *Highly Efficient OLEDs with Phosphorescent Materials*; Wiley-VCH: Weinheim, Germany, 2008.
(7) So, F., Eds. *Organic Electronics*−*Materials, Processing, Devices and Applications*; CRC Press: Boca Raton, FL, 2010.
(8) So, F.; Kido, J.; Burrows, P. *MRS Bull.* **2008**, *33*, 663.
(9) Service, S. F. *Science* **2006**, *310*, 1762.
(10) Walzer, K.; Maennig, B.; Pfeiffer, M.; Leo, K. *Chem. Rev.* **2007**, *107*, 1233.
(11) D'Andrade, B. W.; Forrest, S. R. *Adv. Mater.* **2004**, *16*, 1585.
(12) Kamtekar, K. T.; Monkman, A. P.; Bryce, M. R. *Adv. Mater.* **2010**, *22*, 572.
(13) Wang, Q.; Ma, D. *Chem. Soc. Rev.* **2010**, *39*, 2387.
(14) Baldo, M. A.; Lamansky, S. L.; Burrows, P. E.; Thompson, M. E.; Forrest, S. R. *Appl. Phys. Lett.* **1999**, *75*, 4.
(15) Kawamura, Y.; Goushi, K.; Brooks, J.; Brown, J. J.; Sasabe, H.; Adachi, C. *Appl. Phys. Lett.* **2005**, *86*, 071104.
(16) Schwartz, G.; Reineke, S.; Rosenow, T. C.; Walzer, K.; Leo, K. *Adv. Funct. Mater.* **2009**, *19*, 1319.
(17) Schwartz, G.; Pfeiffer, M.; Reineke, S.; Walzer, K.; Leo, K. *Adv. Mater.* **2007**, *19*, 3672.
(18) Kondakova, M. E.; Deaton, J. C.; Pawlik, T. D.; Giesen, D. J.; Kondakov, D. Y.; Young, R. H.; Royster, T. L.; Comfort, D. L.; Shore, J. D. *J. Appl. Phys.* **2010**, *107*, 014515.
(19) Su, S.-J.; Gonmori, E.; Sasabe, H.; Kido, J. *Adv. Mater.* **2008**, *20*, 4189.
(20) Adachi, C.; Kwong, R. C.; Djurovich, P.; Adamovich, V.; Baldo, M. A.; Thompson, M. E.; Forrest, S. R. *Appl. Phys. Lett.* **2001**, *79*, 2082.
(21) Holmes, R. J.; Forrest, S. R.; Tung, Y.-J.; Kwong, R. C.; Brown, J. J.; Garon, S.; Thompson, M. E. *Appl. Phys. Lett.* **2003**, *82*, 2422.
(22) Tokito, S.; Iijima, T.; Suzuri, Y.; Kita, H.; Tsuzuki, T.; Sato, F. *Appl. Phys. Lett.* **2003**, *83*, 569.
(23) Kido, J.; Ide, N.; Li, Y.-J.; Agata, Y.; Shimizu, H. *IQEC/CLEO-PR* **2005**, CWN1–2.
(24) Sasabe, H.; Gonmori, E.; Chiba, T.; Li, Y.-J.; Tanaka, D.; Su, S.-J.; Takeda, T.; Pu, Y.-J.; Nakayama, K.; Kido, J. *Chem. Mater.* **2008**, *20*, 5951.
(25) Weaver, M. S.; Tung, Y.-J.; D'Andrade, B.; Esler, J.; Brown, J. J.; Lin, C.; Mackenzie, P. B.; Walters, R. W.; Tsai, J.-Y.; Brown, C. S.; Forrest, S. R.; Thompson, M. E. *SID Digest* **2006**, *37*, 127.
(26) Chi, Y.; Chou, P.-T. *Chem. Soc. Rev.* **2010**, *39*, 638.
(27) Yang, C.-H.; Cheng, Y.-M.; Chi, Y.; Hsu, C.-J.; Fang, F.-C.; Wong, K.-T.; Chou, P.-T.; Chang, C.-H.; Tsai, M.-H.; Wu, C.-C. *Angew. Chem., Int. Ed.* **2007**, *46*, 2418.
(28) Chiu, Y.-C.; Hung, J.-Y.; Chi, Y.; Chen, C.-C.; Chang, C.-H.; Wu, C.-C.; Cheng, Y.-M.; Yu, Y.-C.; Lee, G.-H.; Chou, P. T. *Adv. Mater.* **2009**, *21*, 2221.
(29) Chang, C.-F.; Cheng, Y.-M.; Chi, Y.; Chiu, Y.-C.; Lin, C.-C.; Lee, G.-H.; Chou, P.-T.; Chen, C.-C.; Chang, C.-H.; Wu, C.-C. *Angew. Chem., Int. Ed.* **2008**, *47*, 4542.
(30) Jeon, S. O.; Yook, K. S.; Joo, C. W.; Lee, J. Y. *Adv. Funct. Mater.* **2009**, *19*, 3644.
(31) Lo, S.-C.; Shipley, C. P.; Bera, R. N.; Harding, R. E.; Cowley, A. R.; Burn, P. L.; Samuel, I. D. W. *Chem. Mater.* **2006**, *18*, 5119.
(32) Lee, S. J.; Park, K.-M.; Yang, K.; Kang, Y. *Inorg. Chem.* **2009**, *48*, 1030.
(33) Erk, P.; Bold, M.; Egen, M.; Fuchs, E.; Gessner, T.; Kahle, K.; Lennartz, C.; Molt, O.; Nord, S.; Reichelt, H.; Schildknecht, C.; Johannes, H.-H.; Kowalsky, W. *SID Digest* **2006**, *37*, 131.
(34) http://www.universaldisplay.com/default.asp?contentID=604 (accessed November 2010).
(35) Hahn, K.-H. Material developments for plastic and printed electronics. Plenary Lecture given at the 5th Global Plastic Electronics Conference and Exhibition, Dresden, Germany, Octr 27−29, 2009.
(36) Mi, B.-X.; Gao, Z.-Q.; Kiao, Z.-J.; Huang, W.; Chen, C.-H. *Sci. China Chem.* **2010**, *53*, 1679.
(37) Yeh, S.-J.; Wu, M.-F.; Chen, C.-T.; Song, Y.-H.; Chi, Y.; Ho, M.-H.; Hsu, S.-F.; Chen., C. H. *Adv. Mater.* **2005**, *17*, 285.
(38) Tsai, M.-H.; Lin, H.-W.; Su, H.-C.; Ke, T.-H.; Wu, C. C.; Fang, F.-C.; Liao, Y.-L.; Wong, K.-T.; Wu, C.-I. *Adv. Mater.* **2006**, *18*, 1216.

(39) Tsai, M.-H.; Hong, Y.-H.; Chang, C.-H.; Su, H.-C.; Wu, C. C.; Matoliukstyte, A.; Simokaitiene, J.; Grigalevicius, S.; Grazulevicius, J. V.; Hsu, C.-P. *Adv. Mater.* **2007**, *19*, 862.
(40) Shih, P.-I.; Chiang, C.-L.; Dixit, A. K.; Chen, C.-K.; Yuan, M.-C.; Lee, R.-Y.; Chen, C.-T.; Diau, E. W.-G.; Shu, C.-F. *Org. Lett.* **2006**, *8*, 2799.
(41) Wong, K.-T.; Chen, Y.-M.; Lin, Y.-T.; Su, H.-C.; Wu, C. C. *Org. Lett.* **2005**, *7*, 5361.
(42) Whang, D. R.; You, Y.; Kim, S. H.; Jeong, W.-l.; Park, Y.-S.; Kim, J.-J.; Park, S. Y. *Appl. Phys. Lett.* **2007**, *91*, 233501.
(43) Holmes, R. J.; D'Andrade, B. W.; Forrest, S. R.; Ren, X.; Li, J.; Thompson, M. E. *Appl. Phys. Lett.* **2003**, *83*, 3818.
(44) Shih, P.-I.; Chien, C.-H.; Chuang, C.-Y.; Shu, C.-F.; Yang, C.-H.; Chen, J.-H.; Chi, Y. *J. Mater. Chem.* **2007**, *17*, 1692.
(45) Vecchi, P. A.; Padmaperuma, A. B.; Qiao, H.; Sapochak, L. S.; Burrows, P. E. *Org. Lett.* **2006**, *8*, 4211.
(46) Padmaperuma, A. B.; Sapochak, L. S.; Burrows, P. E. *Chem. Mater.* **2006**, *18*, 2389.
(47) Sapochak, L. S.; Padmaperuma, A. B.; Cai, X.; Male, J. L.; Burrows, P. E. *J. Phys. Chem. C* **2008**, *112*, 7989.
(48) Shih, P.-I.; Chien, C.-H.; Wu, F.-I.; Shu, C.-F. *Adv. Funct. Mater.* **2007**, *17*, 3514.
(49) Brunner, K.; van Dijken, A.; Börner, H.; Bastiaansen, J. J. A. M.; Kiggen, N. M. M. M.; Langeveld, B. M. W. *J. Am. Chem. Soc.* **2004**, *126*, 6035.
(50) Huang, S.-P.; Jen, T.-H.; Chen, Y.-C.; Hsiao, A.-E.; Yin, S.-H.; Chen, H.-Y.; Chen, S.-A. *J. Am. Chem. Soc.* **2008**, *130*, 4699.
(51) Baldo, M. A.; Adachi, C.; Forrest, S. R. *Phys. Rev. B* **2000**, *62*, 10967.
(52) Reineke, S.; Walzer, K.; Leo, K. *Phys. Rev. B* **2007**, *75*, 125328.
(53) Reineke, S.; Schwartz, G.; Walzer, K.; Falke, M.; Leo, K. *Appl. Phys. Lett.* **2009**, *94*, 163305.
(54) Reineke, S.; Rosenow, T. C.; Lüssem, B.; Leo, K. *Adv. Mater.* **2010**, *22*, 3189.
(55) Giebink, N. C.; Forrest, S. R. *Phys. Rev. B* **2008**, *77*, 235215.
(56) He, G.; Pfeiffer, M.; Leo, K.; Hofmann, M.; Birnstock, J.; Pudzich, R.; Salbeck, J. *Appl. Phys. Lett.* **2004**, *85*, 3911.
(57) Agata, Y.; Shimizu, H.; Kido, J. *Chem. Lett.* **2007**, *36*, 316.
(58) Watanabe, S.; Kido, J. *Chem. Lett.* **2007**, *36*, 590.
(59) Sasabe, H.; Pu, Y.-J.; Nakayama, K.; Kido, J. *Chem. Commun.* **2009**, 6655.
(60) Su, S.-J.; Sasabe, H.; Takeda, T.; Kido, J. *Chem. Mater.* **2008**, *20*, 1691.
(61) Fukagawa, H.; Yokoyama, N.; Irisa, S.; Tokito, S. Adv. Mater. **2010**, DOI:10.1002/adma.201001221.
(62) Sasabe, H.; Gonmori, E.; Chiba, T.; Pu, Y.-J.; Nakayama, K.; Kido, J. *Asian Conference on Organic Electronics* **2009**, O-13.
(63) Sasabe, H.; Gonmori, E.; Chiba, T.; Pu, Y.-J.; Nakayama, K.; Kido, J. *International Conference on Science and Technology of Synthetic Metals* **2010**, 5P-197.
(64) Kulkarni, A.; Tonzola, C. J.; Babel, A.; Jenekhe, S. A. *Chem. Mater.* **2004**, *16*, 4556.
(65) Hughes, G.; Bryce, M. R. *J. Mater. Chem.* **2005**, *15*, 94.
(66) Tamao, K.; Uchiba, M.; Izumizawa, T.; Furukawa, K.; Yamaguchi, S. *J. Am. Chem. Soc.* **1996**, *118*, 11974.
(67) Murata, H.; Malliaras, G. G.; Uchida, M.; Shen, Y.; Kafafi, Z. H. *Chem. Phys. Lett.* **2001**, *339*, 161.
(68) Ono, K.; Wakida, M.; Saito, K.; Suto, M.; Matsushita, Y.; Naka, S.; Okada, H.; Onnagawa, H. *Chem. Lett.* **2005**, *34*, 1698.
(69) Tanaka, D.; Takeda, T.; Chiba, T.; Watanabe, S.; Kido, J. *Chem. Lett.* **2007**, *36*, 262.
(70) Tanaka, D.; Agata, Y.; Takeda, T.; Watanabe, S.; Kido, J. *Jpn. J. Appl. Phys.* **2007**, *46*, L117.
(71) Tanaka, D.; Sasabe, H.; Li, Y.-J.; Su, S.-J.; Takeda, T.; Kido, J. *Jpn. J. Appl. Phys.* **2007**, *46*, L10.
(72) Sasabe, H.; Chiba, T.; Su, S.-J.; Pu, Y.-J.; Nakayama, K.; Kido, J. *Chem. Commun.* **2008**, 5821.
(73) Su, S.-J.; Tanaka, D.; Li, Y.-J.; Sasabe, H.; Takeda, T.; Kido, J. *Org. Lett.* **2008**, *10*, 941.
(74) Su, S.-J.; Chiba, T.; Takeda, T.; Kido, J. *Adv. Mater.* **2008**, *20*, 2125.
(75) Su, S.-J.; Takahashi, Y.; Chiba, T.; Takeda, T.; Kido, J. *Adv. Funct. Mater.* **2009**, *19*, 1260.
(76) Xiao, L.; Su, S.-J.; Agata, Y.; Lan, H.; Kido, J. *Adv. Mater.* **2009**, *21*, 1271.
(77) Li, Y.-J.; Sasabe, H.; Su, S.-J.; Tanaka, D.; Takeda, T.; Pu, Y.-J.; Kido, J. *Chem. Lett.* **2009**, *38*, 712.
(78) Li, Y.-J.; Sasabe, H.; Su, S.-J.; Tanaka, D.; Takeda, T.; Pu, Y.-J.; Kido, J. *Chem. Lett.* **2010**, *39*, 140.
(79) Su, S.-J.; Sasabe, H.; Pu, Y.-J.; Nakayama, K.; Kido, J. *Adv. Mater.* **2010**, *22*, 3311–3316.
(80) Kido, J.; Gonmori, E.; Ide, N.; Tanaka, D.; Nakayama, K.; Pu, Y.-J. *Proceedings of the Material Research Society Spring 2007 Meeting*; San Francisco, April 9−13, 2007; Materials Research Society: Warrendale, PA, 2007; O6.35.
(81) Sun, Y.; Forrest, S. R. *Nat. Photonics* **2008**, *2*, 483.
(82) Meerheim, R.; Walzer, K.; He, G.; Pfeiffer, M.; Leo, K. *Proc. SPIE* **2006**, *6192*, 61920P.
(83) Kido, J.; Matsumoto, T. *Appl. Phys. Lett.* **1998**, *73*, 2866.
(84) He, G.; Pfeiffer, M.; Leo, K.; Hofmann, M.; Birnstock, J.; Pudzichi, R.; Salbeck, J. *Appl. Phys. Lett.* **2004**, *85*, 3911.
(85) Watanabe, S.; Ide, N.; Kido, J. *Jpn. J. Appl. Phys.* **2007**, *46*, 1186.
(86) Sasabe, H.; Tanaka, D.; Yokoyama, D.; Chiba, T.; Pu, Y.-J.; Nakayama, K.; Yokoyama, M.; Kido, J. Adv. Funct. Mater. **2010**, DOI:10.1002/adfm.201001252.
(87) Winkler, M.; Houk, K. N. *J. Am. Chem. Soc.* **2007**, *129*, 1805.
(88) Meier, C.; Ziener, U.; Landfester, K.; Weihrich, P. *J. Phys. Chem. B* **2005**, *109*, 21015.
(89) Ziener, U. *J. Phys. Chem. B* **2008**, *112*, 14698.
(90) Lin, H.-W.; Lin, C.-L.; Chang, H.-H.; Lin, Y.-T.; Wu, C.-C.; Chen, Y.-M.; Chen, R.-T.; Chien, Y.-Y.; Wong, K.-T. *J. Appl. Phys.* **2004**, *95*, 881.
(91) Yokoyama, D.; Sakaguchi, A.; Suzuki, M.; Adachi, C. *Appl. Phys. Lett.* **2008**, *93*, 173302.
(92) Ichikawa, M.; Kawaguchi, T.; Kobayashi, K.; Miki, T.; Furukawa, K.; Koyama, T.; Taniguchi, Y. *J. Mater. Chem.* **2006**, *16*, 221.
(93) Yokoyama, D.; Sakaguchi, A.; Suzuki, M.; Adachi, C. *Appl. Phys. Lett.* **2009**, *95*, 243303.
(94) Bartels, L. *Nat. Chem.* **2010**, *2*, 87.
(95) Kim, D.; Salman, S.; Coropseanu, V.; Salomon, E.; Padmaperuma, A. B.; Sapochak, L. S.; Kahn, A.; Brédas, J. L. *Chem. Mater.* **2010**, *22*, 247.
(96) Marsal, P.; Avilov, I.; da Silva Filho, D. A.; Brédas, J. L.; Beljonne, D. *Chem. Phys. Lett.* **2004**, *392*, 521.
(97) Avilov, I.; Marsal, P.; Brédas, J. L.; Beljonne *Adv. Mater.* **2004**, *16*, 1624.
(98) http://www.lumiotec.com/
(99) Kido, J.; Matsumoto, T.; Nakada, T.; Endo, J.; Mori, K.; Kawamura, N.; Yokoi, A. *SID Dig.* **2003**, *34*, 964.
(100) Matsumoto, T.; Nakada, T.; Endo, J.; Mori, K.; Kawamura, N.; Yokoi, A.; Kido, J. *SID Dig.* **2003**, *34*, 979.
(101) Kido, J.; Fujita, Y.; Ide, N.; Nakayama, K. *Proceedings of the Materials Research Society Spring 2007 Meeting*; San Francisco, April 9−13, 2007; Materials Research Society: Warrendale, PA, 2007; O10.8.
(102) Takahashi, M.; Pu, Y.-J.; Nakayama, K.; Kido, J. *Proceedings of the Materials Research Society Fall 2008 Meeting*; Boston, Dec 1−5, 2008; Materials Research Society: Warrendale, PA, 2008; G12.7.